ISSN 0126–1533 NOMOR AKREDITASI: 388/AU2/P2MI/04/2012

TEKNOLOGI INDONESIA

LIPI

Volume 39, No. 2, 2016

CONTENTS

Teknologi Indonesia 39 (2) 2016: 81–92

Teknologi Indonesia
LIPI

PRECIPITATION EVENT ANALYSIS USING IMAGE PROCESSING BASED ON THE RAINFALL DETECTION RADAR (RDR) OBSERVATION ON MARCH 9 2014 DURING LANDSLIDE EVENT IN WEST JAVA

Ginaldi Ari Nugroho, Haries Satyawardhana, Erma Yulihastin, Didi Satiadi, Halimurrahman [1]
Center for Atmospheric Sciences and Technology [1]
National Aeronautics and Space – LAPAN
Jln. Dr Djundjunan No.133 Bandung 40173 Indonesia
E-mail: ginaldi.ari@lapan.go.id, ginaldi.lapan@gmail.com

Received: 06-11-2015 Revised: 29-02-2016 Accepted: 02-03-2016

ABSTRACT

A Rainfall Detection Radar (RDR) is a simple weather radar based on marine radar that able is to detect the rainfall within 40 km of range located in Bandung. This system is able to conduct continuous operation, with temporal resolution of 3 minutes with data analysis using an image processing method, to analyze the observation data on March 9, 2014 during the landslide event. The landslides are located 24.6 km southwest from the RDR site. According to observation data, there are 2 large rainfall areas distribution that appear near the landslide location. The second rainfall area is estimated to have initiated the landslide. This second area has two detected object. Object A showed first with maximum size of $\pm$ 6.47 km^2. From the image processing point of view, the object A contributes to the size area of object B. Object B is the second object detected soon after object A appears. Object B has three peaks of its estimated size area with the highest size of $\pm$ 19.4 km^2 occuring in 16.14 LT, and will move towards the southeast affected by local wind leaving the landslide location in 16.37 LT. RDR mean rainfall intensity in radius of 1 km from landslide location on 9 March showed the range value from 0.5–2.5 mm/hour that is located in the east side of the landslide location with the duration over 1 hour.

Keywords: RDR, rainfall, image processing, landslide

ABSTRAK

Radar Deteksi Hujan (RDH) adalah radar cuaca sederhana berdasarkan radar kapal yang mampu mendeteksi hujan dalam jangkauan 40 km yang berada di Bandung. Sistem ini mampu melakukan pengamatan secara terus-menerus dengan resolusi temporal 3 menit dengan analisis data menggunakan metode pemrosesan citra untuk menganalisis data observasi pada kejadian longsor tanggal 9 Maret 2014. Lokasi longsor berjarak 24,6 km dari lokasi RDH dan berdasarkan data pengamatan terdapat 2 area hujan yang berukuran besar yang muncul di dekat lokasi tanah longsor. Area hujan kedua adalah area yang diduga menginisiasi terjadinya tanah longsor. Area hujan ini memiliki 2 objek yang terdeteksi. Objek A muncul pertama kali dengan ukuran maksimum hingga $\pm$ 6.47 km^2. Dari sudut pandang metode pengolahan citra maka objek A memiliki kontribusi terhadap luas dari objek B. Objek B adalah objek kedua yang muncul sesaat setelah munculnya objek A. Objek B memiliki 3 nilai puncak yang mana estimasi luas area hujan berada di nilai maksimum, dengan yang tertinggi terjadi pada 16.14 WIB dengan luas $\pm$ 19.4 km^2 dan akan bergerak menuju arah tenggara dipengaruhi oleh faktor angin lokal dan meningggalkan lokasi longsor pada pukul 16.37 WIB. Intensitas hujan rata-rata RDH pada jarak radius 1 km dari titik lokasi longsor pada tanggal 9 Maret 2014 menunjukkan nilai dengan rentang 0.5–2.5 mm/jam terjadi di bagian timur dari lokasi longsor dengan durasi di atas 1 jam.

Kata kunci: *RDH, hujan, pengolahan citra, longsor*

INTRODUCTION

Indonesia has experienced several disasters during 2014. These disasters include flood, landslide, whirling wind, volcano, etc. Landslides have become the deadliest disaster during this period. The landslide disasters are spread in 12 provinces in Indonesia and West Java has the highest frequency besides Central Java and East Java. [1]

The relation between intensity and also the duration of the rainfall event with the landslide initiation have been investigated by many researcher. One of the primary triggers for landslide event is the rainfall with high intensity and/or long duration.[2] Others suggest that the landslide initiations are more sensitive to high intensity rainfall factor rather than long duration rainfall factor [3]. There are also another parameters that have been investigated which include the cumulative rainfall, previous rainfall, rainfall intensity, and also rainfall duration. [4]

West Java is a province located in the middle of a valley-basin topography, surrounded by mountain and valley. This condition will support the impact of the landslide. Ground based observations are needed to monitor the rainfall event in accordance with landslide initiation. One of this ground based instruments for this observation is the weather radar. Weather radar is capable to detect rainfall distribution based on the reflectivity of the backscattering echo. Long range weather radars have proved to be useful for weather forecasting and qualitative surveillance.

However, weather echoes can only be detected at high altitudes without beam shielding caused by mountain or terrain blockage.[5] There is also a generally decrease of comparison between long range radar and surface precipitation estimates generally along with increasing range detection. [6] For this reason, it is difficult for the operated long range weather radar to conduct monitoring into the area. That is why a new strategy must be proposed by using an affordable instrument that could be installed in this certain area.

A new method using an X-Band radar installed in mountain-valley location have been applied in many countries. One of these examples is the X-band radar in Italy supported by the RSG (Remote Sensing Group) of Polytechnic Turin. This system is an added instrument for precipitation monitoring placed inside the valleys area. This system is able to combine with the long range weather radar.[7] A simple weather radar based on marine radar development has been conducted since 2011. This system called RDR (Rainfall Detection Radar), a simple radar scanner that detects the rainfall within 40 km of range located in Bandung. This system consists of a radar scanner, a radar display, a controller, a signal conditioning unit, a signal processing unit and a computer.[8] System display was plotting the radar digital image based on sampling and quantization process. A static map was used to overlay the reflectivity data and able to calculate the coordination of the reflectivity object [9]. This system is able to conduct continuous operation with temporal resolution of 3 minutes with a good result on validation based on weather radar and rain gauge data.

A new RDR data analysis using an image processing method has been developed. The aim of this paper is to analyze this data analysis based on the observation data in 2014 during the landslide event.

METHODOLOGY

RDR have been developed by LAPAN utilizing a marine radar with improved signal processing acquisition. The ADC count-reflectivity data then converted into rain intensity based on field experiment and observation. Rain object areas were analyzed by using image processing to recognize the shape and width of the object. Edge detection was the first process in the image processing, continued with image segmentation and shape analysis. These processes were then combined in order to find the growth and decay of the rain object.

Rainfall Detection Radar

RDR is a simple marine radar consists of radar scanner and display units, a radar control circuit, a signal conditioning circuit, an Analog to Digital Converter (ADC), and a computer with a

Graphical User Interface (GUI). Clutter map and a developed second clutter filter are designed to extract the rain echo signal from the raw signal. Early studies have been conducted to find the performance and ability to extract the rainfall data. Validations based on field comparison with LAPAN Transportable Gamic Mini Weather Radar (GMWR) have been conducted to find the variable for reflectivity radar output conversion. The sensitivity of this system is lower than that of GMWR with the range from 0–55 dBZ with light and moderate rains from 0–29 dBZ and heavy rain from 30–55 dBZ. [10] There are several weaknesses of this X band radar, this system is very sensitive to rainfall that it will attenuate the radar signal when there is a storm or heavy rainfall. The radar signal cannot penetrate this heavy rainfall so it cannot detect the object behind them.

Reflectivity-rainfall (Z-R) relationship was built to produce reliable radar-based rainfall intensities applying radar reflectivity data in hydrometeorology.[11] The rain intensity R is related to the radar reflection Z based on the connection with the power law. The rainfall amounts can be estimated using this relation via the Z-R relation. [12] Field observations have been conducted from January to March 2014 to find the appropriate Z-R relation with this RDR system.[13] The result showed strong linier relation between RDR data with rain gauge data with a Z-R equation that is now applied to the system.

Rainfall Physical Analysis using Image Processing

The RDR acquisition system will extract the rainfall data and transform into Cartesian coordinate data in a form of matrix and image data. This image data were then processed using image processing to analyze the physical parameter of the rainfall distribution. This process consists of several steps those are edge detection, image segmentation and shape analysis respectively.

Edge detection was the first step to distinguish an object with another object. This technique was to find the position of the object based on horizontal, vertical and their combination of pixel intensity difference.[14] Image segmentation was the second step where each image object then labeled based on its index. Eight connected label method were used by observing the four neighbor pixel with each object area given a different index.[15] This method will detect the amount of rain object area that was detected by the RDR. Shape analysis was the final step where the system will measure the size of each rain object area from the earlier method then find the highest area that usually possesses large amount of raindrops. This highest area will be marked and observed for its growth/decay and also its movement. Optical flow is the distribution of apparent velocities of movement of brightness patterns in an image. Horn-Schunk optical flow is the global variation method of optical flow algorithm using quantization of image sequences.[16] This image processing systems were then applied to analyze the rain area and duration in a landslide event that occured during observation on March 9th 2014.

RESULTS AND DISCUSSION

Based on National Agency for Disaster Management (*Badan Nasional Penanggulangan Bencana*-BNPB) data, there were several landslides occurred during February until March 2014, in which three of them happened around West Java within radar scope. These disasters were dominantly caused by unstable land structure and also rainfall. Then, an attempt was made to analyza rainfall factor by the RDR observation data among those disaster, with the location and the casualties are stated in Table 1.

Table 1. Landslide Location

Date	Location	latitude	Longitude	Losses	Explanation
9-3-2014	Kp. Lampengan Ds.Wangunsari Kec. Sidangkerta Kab. Bandung Barat Prov. Jawa Bara	-7,03362	107,414	6 house damage	Heavy rainfall with unstable land structure.

(Source: BNPB, 2014)

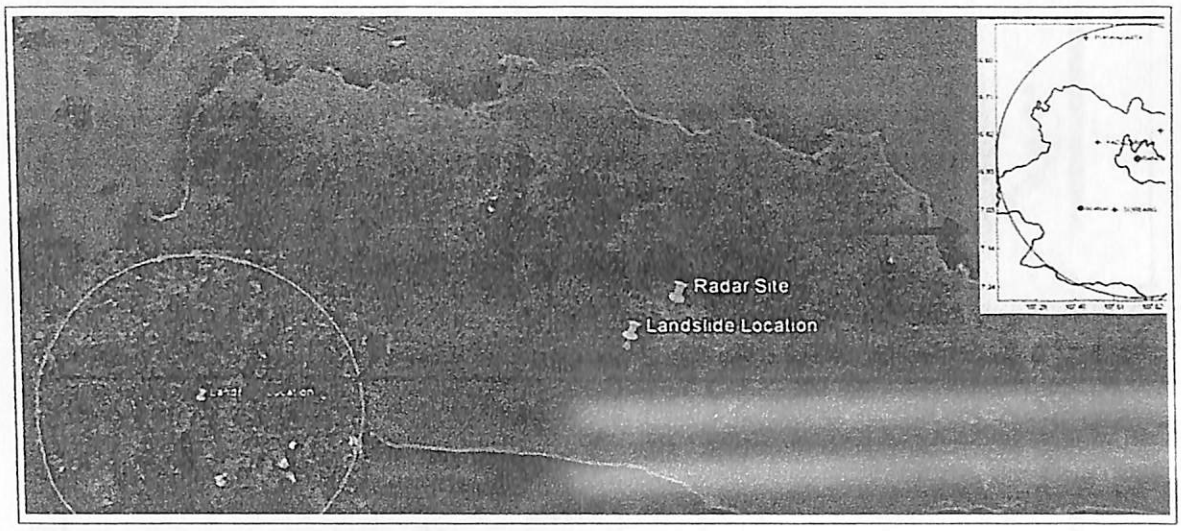

Figure 1. Location Observed in Google Earth

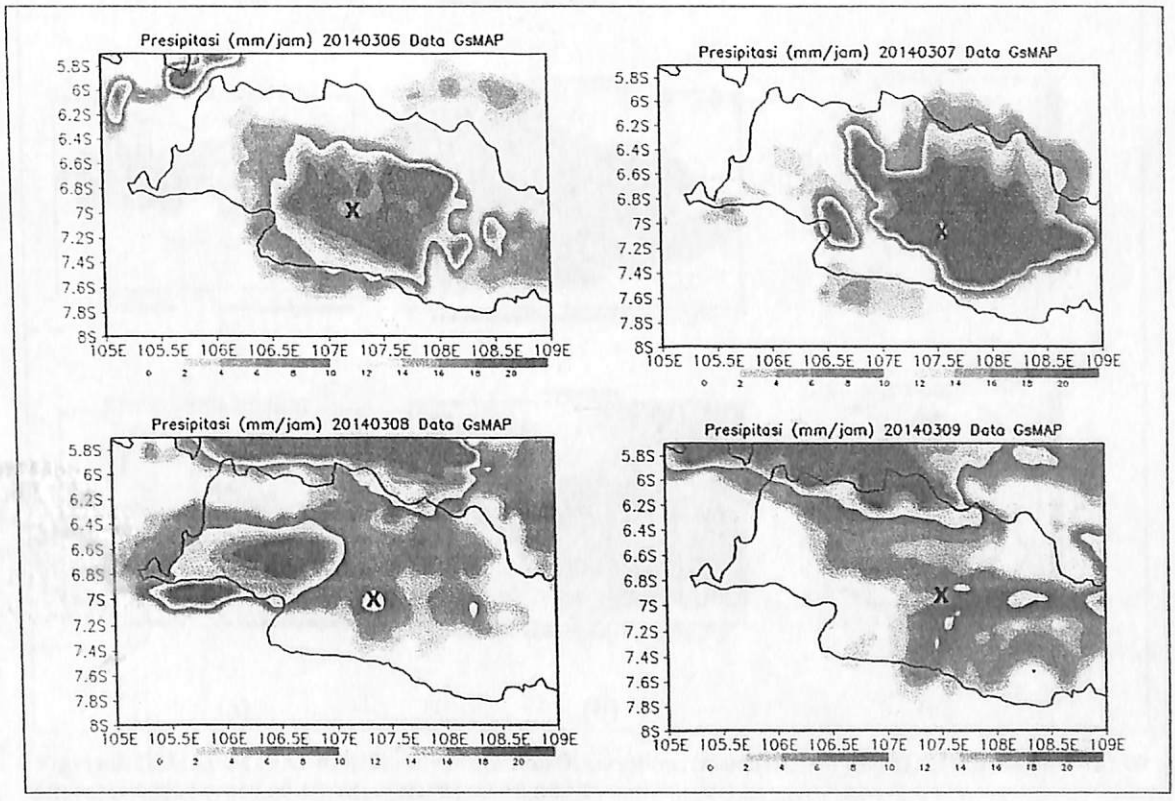

Figure 2. Daily Average of Rainfall 6-9 March 2014, based on GsMAP Satellite Observation

The landslide is located 24.6 km southwest from the RDR site. This disaster was recorded in 16.20 LT (Local Time) at Kp. Lampengan Ds.Wangunsari Kec. Sidangkerta Kab. West Bandung West Java Province. The terrain location observed from Google Earth (insert on Figure 1) has an elevation of 844 meter above sea level with the surrounded areas that have a different elevation where in the east and south side is relatively ascended (slope forward), while the west side is relatively constant and the north side is relatively descended.

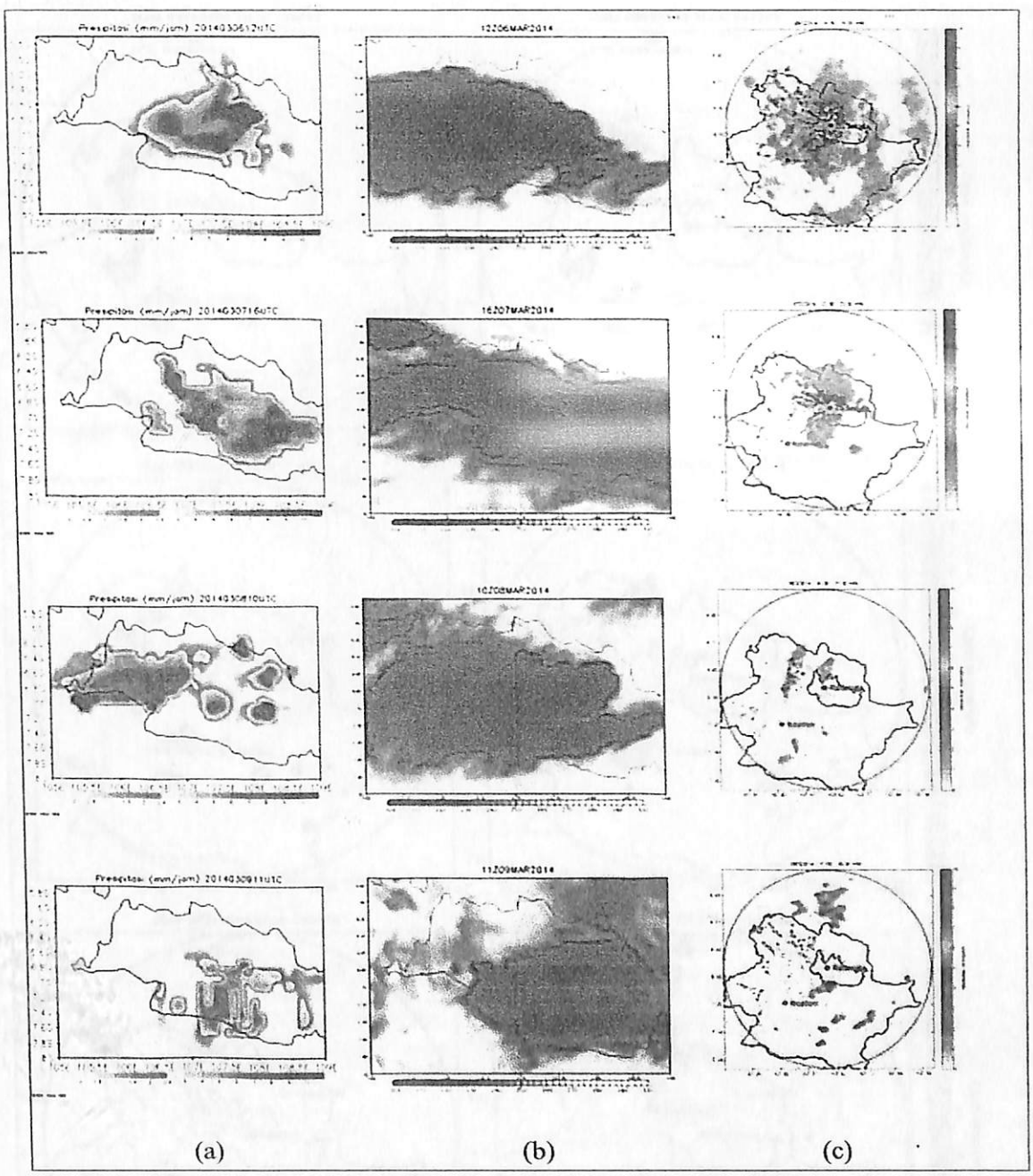

Figure 3. GSMAP-MTSAT-RDR Hourly Maximum Observation , (a) 06032014 – 19.00 LT, (b) 07032014 – 23.00 LT, (c) 08032014 – 17.00 LT, (d) 09032014 – 18.00 LT.

Before continuing with the research, GSMAP (Global Satellite Mapping of Precipitation) data were used to see if there were any precipitation events on the day of the attempt and the previous three days. GSMAP is a project to study the production of a high-precision, high-resolution global precipitation map using satellite data.[17–20]

Figure 2 is the daily GSMAP of precipitation intensity observation data from March 6–9, 2014 around Java Island. Focused on West Java region, there were precipitation intensity in this area. The precipitation also covered the landslide area

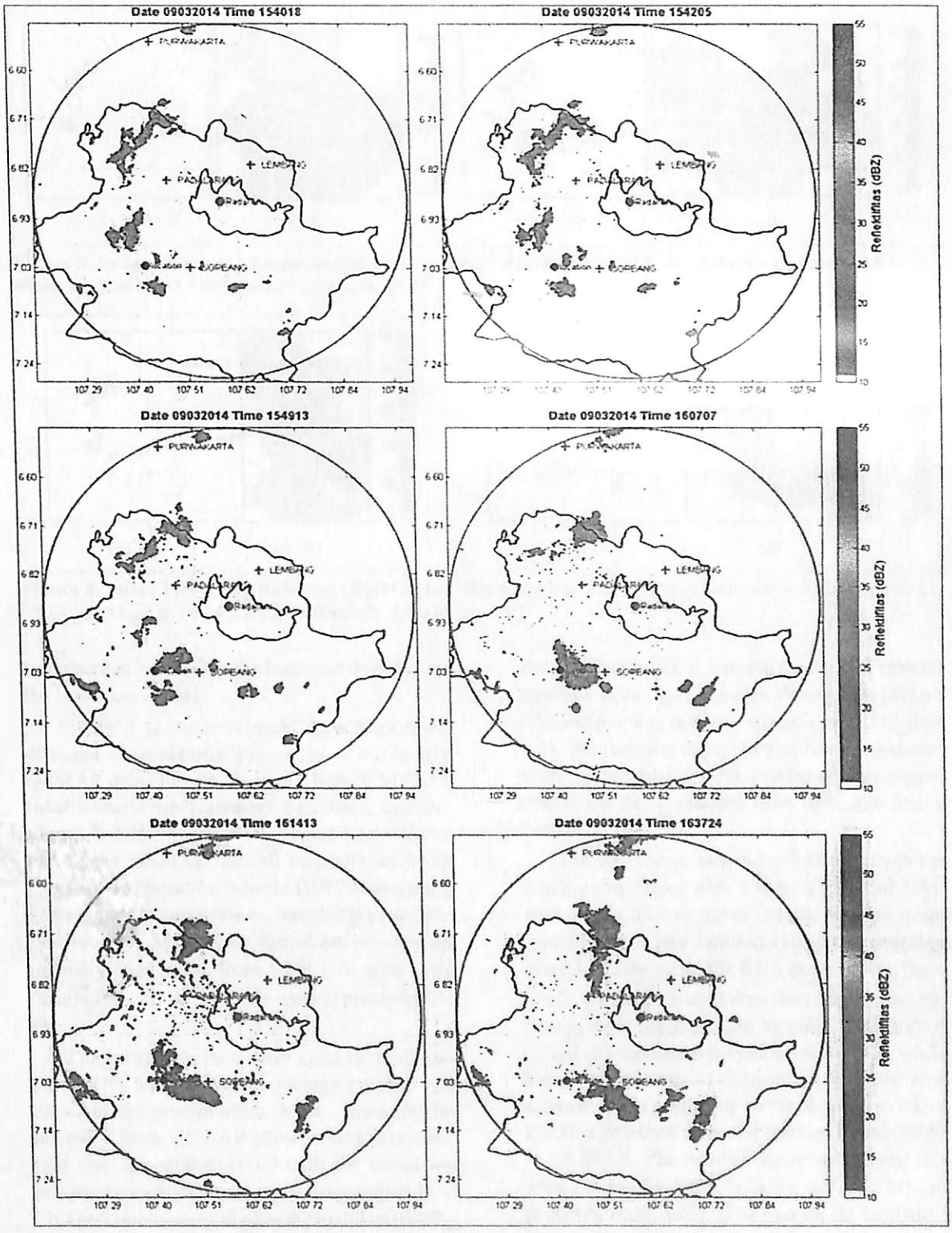

Figure 4. Second Area Object of Rainfall Detected by RDR

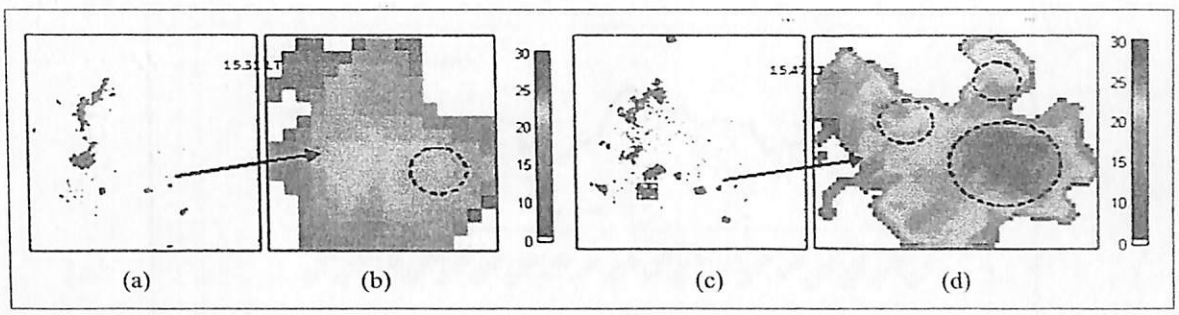

Figure 5. Image Processing Result on Object A, (a) Object Mark in 15.31 LT, (b) Reflectivity Area in 15.31, (c) object mark in 15.47, (d) Reflectivity area in 15.47

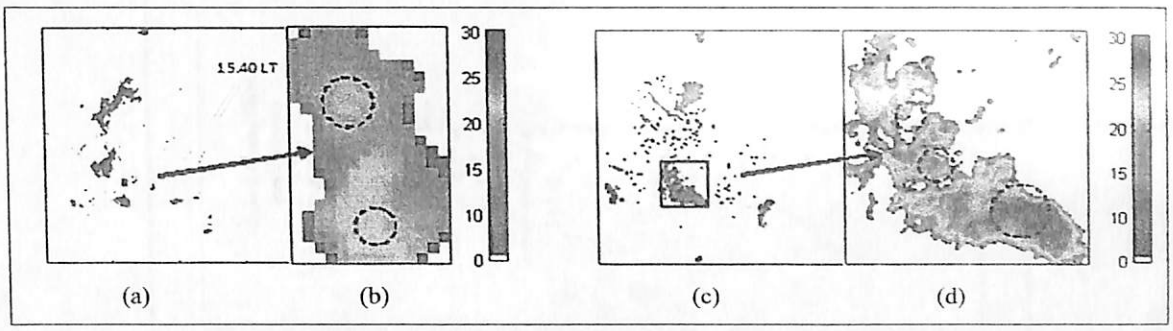

Figure 6. Image Processing Result on Object B, (a) Object Mark in 15.40 LT, (b) Reflectivity Area in 15.40 LT, (c) Object Mark in 16.14 LT, (d) Reflectivity Area in 16.14 LT

(represent in X mark) in the last three days before the landslide occurs.

Figure 3 is the maximum data from three different observations. Figure 3a is the hourly GSMAP data, Figure 3b is the hourly MTSAT (Multifunctional Transport Satellite), and the Figure 3c is the hourly RDR average data. Comparing the GSMAP rainfall intensity with the cloud top temperature from MTSAT observation will support the analysis on the global precipitation occasion. Meanwhile, the reflectivity-rainfall intensity conversion from RDR will give more detailed (local) information on this precipitation event.

The maximum data were used in this comparison to have a wide coverage (global and local) of the precipitation event. Precipitation intensity from GSMAP showed that precipitation area are well-covered with the cloud top temperature which possesses a low temperature. This precipitation occured in the mainland during the afternoon until the evening. The circle area represented the RDR coverage compared with the GSMAP and MTSAT. From this comparison, it showed that in RDR there were several rainfall intensity areas that occured during this period. Although it was difficult to compare RDR data with the satellite data, they all confirmed that there were precipitation events on this region during the days, ranging from light into heavy rainfall.

The RDR observed the reflectivity from the precipitation echo with a scan method of horizontal scan, 0.8 us pulse length, 600 Hz pulse repetition rate, and 3 minutes temporal sampling resolution. Based on the RDR observation, there were two large rainfall area distribution that appeared near the landslide location on Figure 4 (Black dot represents the landslide location, while Red dot represents RDR location). The first area appears in the north side of the location in 14.48 LT. This area then grew and reached its maximum at 15.24 LT. The nearest distance between this area and the landslide location are 4.02 km, so probably there was less impact on the landslide. Meanwhile, the second area appeared in the east and southeast of the location at 15.33 LT. These areas were observed very near with the landslide

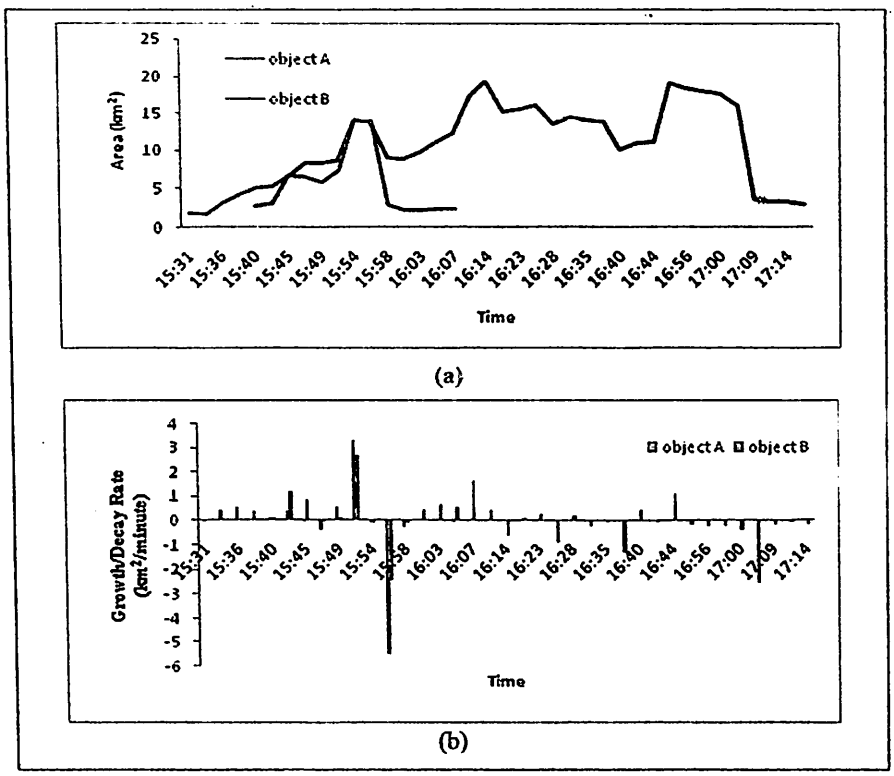

Figure 7. Comparison of Two Object, (a) Area, (b) Growth/Decay rate

location (less than 1km) with two detected objects (Figure 4) as a primary object sample (object A and object B).

Using an image processing method, the two object were analyzed to measure its intensity, maximum area, growth/decay rate and also the vector movement. The first object (Object A) detected in 15.31 LT at coordinate 107.44729^0 E and 7.075134^0 S (Figure. 5a). This object possessed a proximity area of 1.65 km^2, average reflectivity of 17.9 dBZ. The reflectivity distribution are shown in Figure. 5b where there was a single maximum area inside it. This object then grew, reaching its maximum with an area of 6.47 km^2, average reflectivity of 20 dBZ in 15.47 LT (Figure 5c). The maximum area were increased into three maximum areas (Figure. 5d). This object will decay in 16.07 LT.

Second object (object B) appeared at 107.45053° E and 7.020105° S in 15.40 LT (Figure 6a). This object possessed an area of 2.69 km^2, average reflectivity 18.1 dBZ with the area were shown with two maximum areas inside it (Figure 6b). This object will grow rapidly until 16.14 LT (Figure 6c) with the total area estimate of 19.4 km^2 and reflectivity average of 20.4 dBZ (Figure 6d).

Comparison of area and growth/decay rate between the object A and the object B are in Figure 7a and 7b respectively. The object B has a higher area rather than the object A. Using the shape analysis, these two objects seemed to combine each other in 15.54 LT and separated in 15.58 LT. The object B also has three maximum peak where the highest peak was the one that started to drift into the southeast. Object B has lower growth rate but a longer lifetime rather than object A.

The movement of this object are shown in the pixel velocity vector. By using optical flow, it will get the pixel velocity vector based on Horn-Schunk Method. Before the object were combined, the expand growth of these two objects stretched to all direction in the (Figure 8a). Although the reflectivity intensity from these two objects were lower than 40 dB for threshold

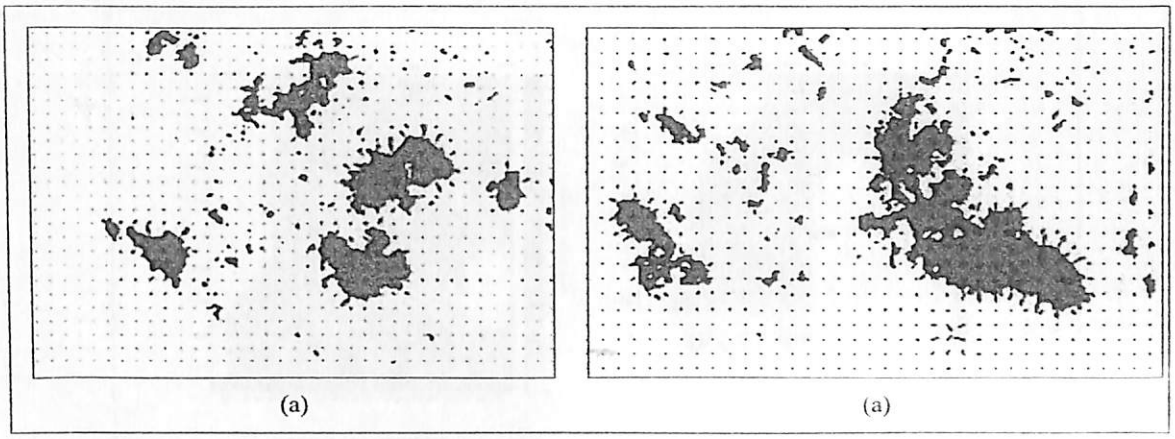

Figure 8. Vector Movement Object A and B , (a) 15.47 LT, (b) 16.14 LT

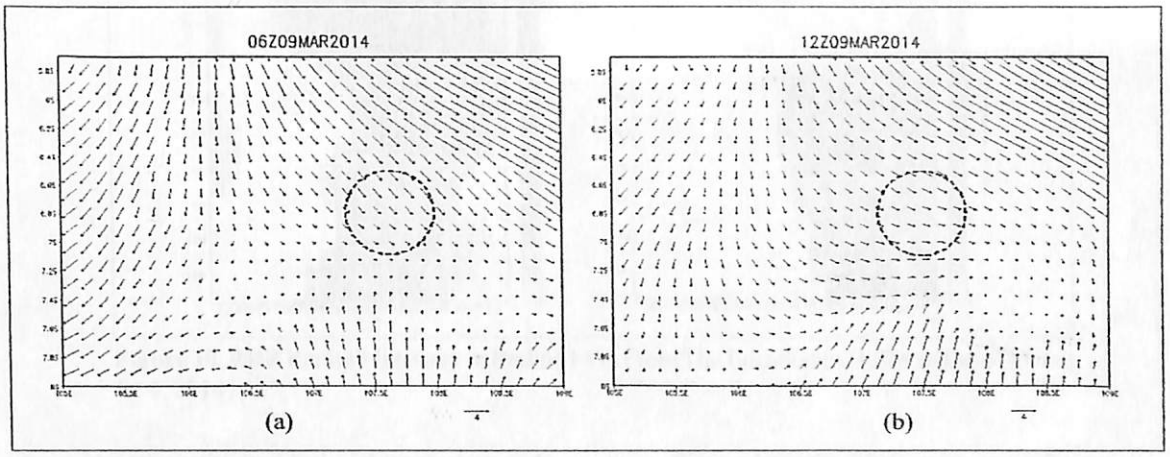

Figure 9. Wind Vector ERA-Interim model on 9 March 2014, (a) 13.00 LT, (b) 19.00 LT

Table 2. Estimated Precipitation Duration

Date	RDR	Duration	GSMAP	Duration
06/03/2014	17.07 – 17.46	0.38	16.00 – 24.00	6
	18.43 – 19.51	1.08		
07/03/2014	14.13 – 15.40	1.17	13.00 – 15.00	2
			17.00 – 24.00	7
08/03/2014	14.19 – 15.04	1.44	00.00 – 04.00	4
			16.00 – 19.00	3
09/03/2014	15.47 – 16.37	1.49	16.00 – 19.00	3

of convective type,[21] but from this stretching movement with steady location it can be assumed that these two objects have a convective type of precipitation. The growth of object A was expanded until reaching its maximum and decay rapidly, while object B will continue to grow. Object B then will drift towards the southeast direction starting in 16.21 LT and decay in 17.16 LT (Figure 8b).

This movement were confirmed with the 10 meter above surface wind vector from ERA-Interim data from ECMWF model[22] with resolution 0.1250 or + 12.5 km with 6 hours of temporal resolution (Figure.9). The circle area was the wind vector data within the RDR range

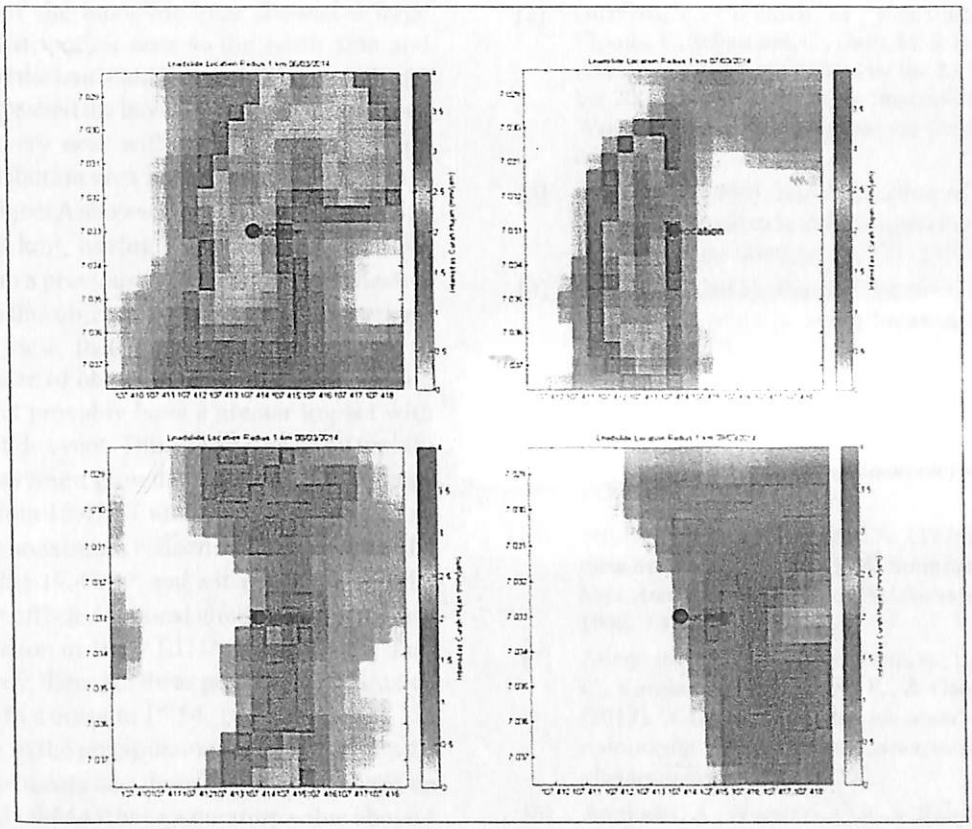

Figure 10. RDR Rainfall Intensity in Radius 1 km From The Location in Different Days (March 6 - 9, 2014)

scope. North westerly wind and westerly wind were spotted in 13.00 LT and 19.00 LT. From the RDR and ERA data, it showed that local factors were affecting this rainfall movement although the global movement showed from GSMAP were moving towards the southwest.

Focus on the duration of the precipitation event around the landslide area within this 4 days period based on the RDR and the GSMAP data are described in Table 2. The duration from both data have different variation but showed above 1 hour of precipitation event. Although GSMAP data have low resolution (0.1° or $\pm$ 10 km), but it gave the information that the RDR cannot handle such kind of precipitation where heavy precipitation are located near the RDR site (precipitation event from 7 to 8 March) due to attenuation. This attenuation will block the radar beam so that it cannot detect precipitation in the landslide area at those period.

Figure 10 is the RDR mean rainfall intensity from the landslide center point location (black-green circle) towards radius of 1 km (324 pixel) in 4 days period. More spread rainfall intensity were spotted in March 6, 2014, but in March 9, 2014 the mean rainfall intensity range from 0.5–2.5 mm/hour were located in the east side of the landslide.

CONCLUSION

Landslide event on 9 March 2014 are analyzed using the RDR image processing method based on the rainfall factor. Verification on the existence of the precipitation event are confirmed using GSMAP and MTSAT data from 6 to 9 March in 2014. Although it is difficult to compare RDR data with the satellite data, but they all confirm that there are precipitation event on this region during this period ranging from light into heavy rainfall. Detailed analysis on the precipitation

object near the landslide area showed 2 large rainfall distribution area in the north side and eastside of the landslide location. The eastside object are expected the have a landslide impact since detected very near with the landslide location. This distribution area have two object (object A and B), object A showed first with maximum size of ± 6.47 km², having 3 maximum reflectivity value from a previous of one maximum reflectivity inside this object. From the image processing point of view, the object A are contributed to the area size of object B. Object B is the second object that probably have a greater impact with the landslide event. This object will grow rapidly with an average growth rate up to ± 0.45 km²/ minute from 15.42 LT until 16.14 LT. This object has three maximum reflectivity value when the size reach ± 19.4 km², and will move towards the southeast affected by local wind leaving the landslide location in 16.37 LT. During this time until fully decay, there are three peaks of its estimated size area that occur in 15.54, 16.14, and 16.51 LT. Duration of the precipitation event at the time the landslide occurs and three days before based on RDR and GSMAP have a duration value above 1 hour. More detail on rainfall intensity in radius of 1 km from landslide location showed that spread rainfall intensity were spotted on 6 March, but on 9 March the mean rainfall intensity range from 0.5–2.5 mm/hour were located in the east side of the landslide. In the future, this system will be expanded in order to forecast the rain object in short-term period. This short term forecast will gave an early warning for incoming rainfall and will gave benefit to the authority or the institution that concerned with hydro meteorological disaster.

ACKNOWLEDGEMENT

This research was funded by the SINAS (Sistem Inovasi Nasional) program from State Ministry of Research and Technology in 2015.

REFERENCES

[1] Badan Nasional Penanggulangan Bencana. (2014). *Info bencana edisi Desember 2014*, Tim Pusdatinmas BNPB, www.bnpb.go.id, Accessed on 21 July 2015.

[2] Guzzetti, F., Cardinali, M., Reichenbach, P., Cipolla, F., Sebastiani, C., Galli, M. & Salvati, P. (2004). Landslides triggered by the 23 November 2000 rainfall event in the Imperia Province, Western Liguria, Italy. *Engineering Geology, 73*, 229–245.

[3] Crosta, G. (1998). Regionalization of rainfall threshold: An aid to landslide hazard evaluation. *Environmental Geology, 35*, 131–145.

[4] Hasnawir. (2012). Rainfall intensity induced shallow landslide in South Sulawesi. *Jurnal Penelitian Kehutanan Wallacea, 1*(1), 62–73.

[5] Gabella, M., & Perona, G. (1998). Simulation of the orographic influence on weather radar using a geometric-optics approach. *Journal of Atmospheric and Oceanic Technology, 15*(6), 1485–1494.

[6] Wilson, J.W. & Brandles, E.A. (1979). Radar measurement of rainfall: A Summary. *Bulletin American Meteorological Society, 60*(9), 1048–1078.

[7] Allegretti, M., Bertoldo, S., Prato, A., Lucianaz, C., Rorato, O., Notarpietro, R., & Gabella, M. (2012). X-band mini radar for observing and monitoring rainfall events. *Atmospheric and climate sciences, 2*, 290–297.

[8] Awaludin, A., Nugroho, G.A, & Rahayu, S.A. (2013). Analisis kemampuan radar navigasi laut Furuno 1932 mark II untuk pemantauan intensitas hujan. *Jurnal Sains Dirgantara, 10*(2), 90–103

[9] Nugroho, G.A., & Awaludin, A. (2014). Mapping method development using digital image processing to calibrate rainfall radar image. *Prosiding Internasional 17th SIPTEKGAN.*

[10] Nugroho, G.A., Munir, M.M., & Khairurrijal. (2014). A computer-based marine automatic radar for rain detection. *Applied Mechanics and Materials, 771*, 9–12.

[11] Ciach, G.J. (1999). Radar-rain gauge comparisons under observational uncertainties. *Journal of applied meteorology, 38*(10), 1519–1525.

[12] Battan, L.J. (1973). *Radar observation of the atmosphere.* Chicago: The University of Chicago Press.

[13] Nugoho, G.A., Awaludin, A., & Rahayu, S,A. (2014). Hasil pengamatan scanner hujan dan AWS pada kejadian hujan tanggal 2–3 Maret 2014 di daerah Bandung dan sekitarnya. *Buku Variabilitas Cuaca dan Iklim di Indonesia*, ISBN 978-979-1458-81-8.

[14] Purnomo, M. H,. & Muntasa, A, (2010). *Konsep pengolahan citra digital dan ekstraksi fitur.* Yogyakarta: Graha Ilmu Yogyakarta, ISBN: 978-979-756-682-1.

[15] Putra, D. (2010). *Pengolahan citra digital.* Yogyakarta: Penerbit ANDI. ISBN 978-979-29-1443-6.

[16] Horn, B., & Schunck, B. (1981). Determining optical flow. *Artificial Intelligence, 17,* 185–203.

[17] Okamoto, K., Iguchi, T., Takahashi, N., Iwanami, K., & Ushio, T. (2005). The Global Satellite Mapping of Precipitation (GSMaP) project. *25th IGARSS Proceedings,* 3414–3416.

[18] Kubota, T., Shige, S., Hashizume, H., Aonashi, K., Takahashi, N., Seto, S., Hirose, M., Takayabu, Y.N., Nakagawa, K., Iwanami, K., Ushio, T., Kachi, M., & Okamoto, K. (2007). Global Precipitation Map using Satelliteborne Microwave Radiometers by the GSMaP Project : Production and Validation. *IEEE Trans. Geosci. Remote Sens, 45*(7), 2259–2275.

[19] Aonashi, K., Awaka, J., Hirose, M., Kozu, T., Kubota, T., Liu, G., Shige, S., Kida, S., Seto, S., Takahashi, N., & Takayabu, Y.N. (2009). GSMaP passive, microwave precipitation retrieval algorithm: Algorithm description and validation. *J. Meteor. Soc. Japan, 87A,* 119–136.

[20] Ushio, T., Kubota, T., Shige, S., Okamoto, K., Aonashi, K., Inoue, T., Takahashi, N., Iguchi, T., Kachi, M., Oki, R., Morimoto, T., & Kawasaki, Z. (2009). A Kalman filter approach to the Global Satellite Mapping of Precipitation (GSMaP) from combined passive microwave and infrared radiometric data. *J. Meteor. Soc. Japan, 87A,* 137–151.

[21] Steiner, M., Houze, Jr. R. A., & Yuter, S.E. (1995). Climatological characterization of three dimensional storm structure from operational radar and rain gauge data. *Journal of applied meteorology, 34,* 1978–2007.

[22] ERA Interim Daily Data. (2015). http://apps.ecmwf.int/datasets/data/interim-full-daily diakses tanggal 28 October 2015.